4ICEGE Thessaloniki-GREECE 2007

4th International Conference on
Earthquake Geotechnical Engineering
June 25-28, 2007
Paper No.1147

STOCHASTIC FINITE-FAULT STRONG GROUND-MOTION SIMULATION OF THE 22 FEBRUARY 2005 (MW 6.4) ZARAND (CENTRAL IRAN) EARTHQUAKE

Hamid ZAFARANI [1], Asadollah NOORZAD[2], Khosro BARGI[3]

ABSTRACT

The stochastic method for finite faults is applied to simulate strong ground motion from the 22 February 2005, moment magnitude M 6.4 Zarand (central Iran) earthquake. In this approach, the ground-motion amplitudes are simulated as a summation of stochastic point sources. The length of the fault was taken as 14 km and its width as 10 km, and the fault plane was divided into 4×3 elements. A uniform slip-distribution model is used to asses the source effect. The fault plane strikes 270˚ (clockwise from north) and dips 67˚ to the north. The depth of 9 km is employed for the earthquake hypocenter. The horizontal acceleration records of nine stations with epicentral distances less than 80 km from the Building and Housing Research Center of Iran (BHRC) database were included in the simulations. The strong motion simulations are performed using model parameters based on the results of previous studies, and looking for value of the radiation-strength factor (*sfact*) that gave the minimum model bias of the acceleration response spectra. We found that *sfact*=1.4 (for a representative value of stress drop parameter, $\Delta\sigma =$ 50 bars) provided the best fit to the observed response spectra and peak ground acceleration (PGA). In conclusion, we found that the overall agreement between simulated and observed waveforms and spectra is quite striking. The simulation parameters obtained in this study can be used to asses the strong-motion level at a much larger number of sites, where no record is available, to investigate how different characteristics of motion affected damage distribution in the Zarand region.

Keywords: Stochastic finite-fault modeling; Ground motion simulation; Zarand earthquake; Iran

INTRODUCTION

The Iranian plateau, located along the Alpine-Himalayan orogenic belt, is one of the most highly seismic regions of the world. Many devasting earthquakes have occurred during the long history of this ancient country (Berberian & Yeats, 2001). Continental coverage of about 35 mm/yr between the Eurasian and Arabian plates is absorbed in Iran by strike-slip and reverse faults (Jackson et al., 1995). However the active deformation is not uniformly distributed and no single fault accommodates a large percentage of plate convergence (Berberian & Yeats, 2001). The most active seismic zones, in decreasing order of activity, are: Zagros, Alborz and East-Central Iran (Berberian, 1976; Takin, 1972). Central Iran is characterized by scattered seismic activity with large magnitude earthquakes, long recurrence periods and seismic gaps along several Quaternary faults. The earthquakes in the zone are generally shallow and are usually associated with surface faulting (Berberian, 1976; 1979).

On 22 February 2005 at 02:25 GMT, a shallow destructive earthquake of Mw 6.4 occurred east of Zarand town (central Iran), about 60 km north of the city of Kerman, the provincial capital. The earthquake demolished much of the town and other neighbouring villages. Number of victims reached more than 600 people. Many of the structures in the region were poorly designed mud-brick

[1]PhD Candidate, Department of Civil Engineering, University of Tehran, Iran, Email: zaferani@ut.ac.ir
[2]Assistant Professor, Department of Civil Engineering, University of Tehran, Iran.
[3]Associate Professor, Department of Civil Engineering, University of Tehran, Iran.

constructions that collapsed quickly on sleeping inhabitants. The focal mechanism solutions as well as field observation show that this earthquake involved thrust faulting on a plane striking nearly east-west and dipping towards the north (Talebian et al., 2006). Twenty seven strong-motion instruments (SSA-2 accelerometers) of the BHRC located mainly within the state of Kerman recorded the mainshock. The availability of these data, as well as the sufficient knowledge of the geometry of the causative fault, also destructiveness of this event was the most important motivation for simulating these acceleration waveforms.

According to Talebian et al. (2006), the 2005 Zarand earthquake involved reverse faulting, unlike the strike-slip faulting responsible for the earlier recent earthquakes in this zone. It had a northward dip of about 67˚, which is steep even for reverse faults (Talebian et al, 2006).

In this article, we use strong-motion records from 9 stations azimuthally well distributed to find the necessary source and propagation parameters for the stochastic model proposed by Beresnev and Atkinson (1997, 1998a).

DATA

Figure 1 shows the distribution of the 10 stations selected for the analyses and the location of the earthquake epicenter. All of the available records were taken from BHRC Database. We selected records from stations located on free-field sites with clear P- and S-wave arrivals and a signal-to-noise ratio greater than 3. Table 1 lists the coordinates and site characteristics of these stations. Figure 1 also shows the rupture area (gridded rectangle), epicentral location and the focal mechanism of the event.

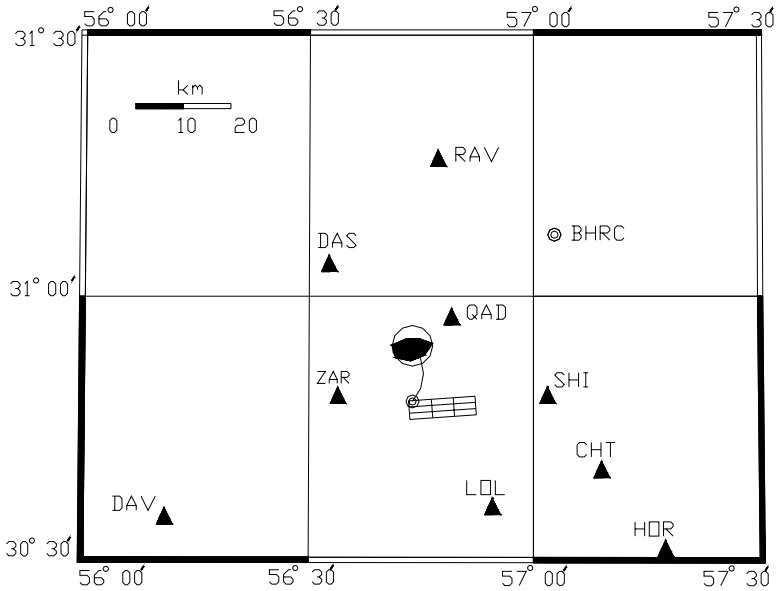

Figure 1. Epicentral location of the 22 February, 2005 (Mw 6.4) earthquake and distribution of stations used. The focal mechanism and the rupture area are also shown.

The recording instruments are digital accelerographs (Kinemetrics SSA-2), installed at distances ranging from 16 to 236 km with respect to the epicenter of the examined earthquake. The maximum peak ground acceleration as much as 510 cm/s/s was recorded at the Shirinrood Dam station.
Detailed information on the locations (Fig. 1) and the geological conditions at the installation sites, as well as PGA values recorded during the examined earthquake are given in Table 1.

Table 1. Recording characteristics of the strong-motion stations used

Code	Station Name	Latitude	Longitude	Epicentral Distance (km)	Site Class	PGA/L (cm/s/s)	PGA/T (cm/s/s)
CHT	Chatrood	30.60	56.91	28	hard rock	55	87
DAS	Dasht-e-Khak	31.06	56.55	33	hard rock	48	60
DAV	Davaran	30.58	56.19	58	rock	60	47
HOR	Horjand	30.67	57.15	42	hard rock	52	44
LOL	Deh-e-Loulo	30.52	57.29	61	rock	50	31
QAD	Qadrooni Dam	30.96	56.82	19	rock	212	142
RAV	Ravar	37.21	50.03	51	soil	118	70
SHI	Shirinrood Dam	30.811	57.031	28	stiff soil	500	196
ZAR	Zarand	30.81	56.57	16	soil	308	244

SIMULATION METHOD AND PARAMETERS

The procedure used for the generation of high frequency components of ground motion is the widely applied stochastic finite-fault method of Beresnev and Atkinson (1997). They assumed that a main earthquake of seismic moment M_0 can be represented by $n = M_0/m_0$ sub-sources, where the seismic moment of each sub-source is

$$m_0 = \Delta\sigma \Delta l^3 \tag{1}$$

where $\Delta\sigma$ is the stress drop that takes place on each sub-source and Δl is the sub-source dimension. Using kinematic rupture modeling, defining hypocenter and rupture velocity (which is a fairly stable parameter) on the fault, and assuming radial propagation from the hypocenter, one can construct the total motion at each point as the sum of the contribution from all sub-events considering appropriate triggering time (triggering is assumed when the rupture front passes through the sub-fault) for each one. Each sub-source radiates elastic waves according to the ω^2 spectrum with corner frequency

$$f_c = \frac{(\frac{yz}{\pi})\beta}{\Delta l}, \tag{2}$$

where $y = v/\beta$ is the ratio of rupture velocity to shear velocity in the source region and z is an arbitrary factor controlling the high-frequency radiation. This factor is related to the maximum slip rate, v_m , on the fault in the following way

$$v_m = (\frac{2yz}{e})(\frac{\Delta\sigma}{\rho\beta}), \tag{3}$$

where e is the base of the natural logarithm and ρ is the density of the medium. The value of z is the product of a standard factor of 1.68, and the *sfact* parameter. The *sfact* parameter controls the strength of fault radiation at frequencies higher than the corner frequency of subfaults and changes between 0.5 and 2.0 (Beresnev & Atkinson, 1997).

Defining the input parameters consisting of fault geometry, target moment magnitude, sub-event size, slip velocity on the fault and regional properties defining path effects, one can determine ω^2 source spectrum of each subevent, which after multiplying by a normalized limited-duration Gaussian noise, takes the stochastic characteristics of real motion.
In order to apply the point source approximation used by the code, we divided the fault plane into subfaults. According to Beresnev and Atkinson (2002), the sub-fault size increases linearly with moment magnitude, in accordance with the relationship:

$$\log \Delta l = -2 + 0.4M \; (4 \le M \le 8) \tag{4}$$

where Δl is the subfault length and M (6.4) is the magnitude. This relationship is regionally independent (Roumelioti & Beresnev, 2003). Assuming that $\Delta l \approx \Delta w$, where Δw is the subfault width, we divided the rupture area into 4×3 subfaults. Following the approach taken by Beresnev and Atkinson (2002), the fault was assigned a homogeneous slip, since the details of the slip distribution are not well constrained and it has been found not to affect the accuracy of the predictions on average (Beresnev & Atkinson, 1998b). The dimensions and orientation of the fault plane are based on the model proposed by Talebian et al. (2006), which is consistent with the spatial distribution of aftershocks and field observations. The fault plane strikes 270˚ (clockwise from north) and dips 67˚ to the north (Talebian et al., 2006). This value appears more compatible with the field observations in comparison with Harvard CMT solution that determined a strike of 261˚. The depth of 9 km is employed for earthquake hypocenter (Talebian et al., 2006). The hypocenter was placed at the north-west, bottom half of the fault. A length of 14 km is selected according to the surface rupture length observed in the field (Talebian et al., 2006).
The anelastic attenuation model was represented by a mean frequency-dependent quality factor $Q = 130 f^{0.94}$, derived from studies of S-wave attenuation in the region. For the geometric spreading, we applied a geometric spreading operator of R^{-1} for the stations with epicentral distances less equal 100 km (Aki & Richards, 1980). The material properties are described by density, ρ , and shear-wave velocity, β , and the values adopted for them are 2.8 g/cm^3 and 3.5 km/s, respectively in accordance to Sadeghi et al. (2006) . The rupture velocity is taken as depth independent at a value of 0.8 times the shear-wave velocity (Beresnev & Atkinson, 1997). In our calibrated model, the sub-event stress drop is a fixed parameter (set at 50 bars for all simulations) and is used only to determine the moment associated with each sub-fault as in Atkinson and Beresnev (2002). All the parameters used are summarized in Table 2.

Unfortunately, there is no information concerning the actual amplification factors in the region. This limitation could be overcome by the use of mean amplification factors based on a gross characterization of the site class (Roumelioti & Kiratzi, 2002). The classification of the sites was performed following the scheme proposed by Zare et al. (1999), which is based on the mean horizontal to vertical spectral ratios. The amplification factors employed for each site category are given by Boore and Joyner (1997).
To calibrate the input parameters of the model, the bias was defined as:

$$E(f) = \frac{1}{n} \sum_{i=1}^{n} \log\left(\frac{PSA(f)_{obs}}{PSA(f)_{sim}}\right)_i, \tag{5}$$

where n is the number of stations and $PSA(f)_{obs}$ are the response acceleration spectra. The simulated $PSA(f)_{sim}$ was obtained using the finite-fault radiation simulation code FINSIM (Beresnev & Atkinson, 1998a), which its applicability to ground-motion prediction in various tectonic environments has been verified in several recent studies (Beresnev & Atkinson, 1998b; Berardi et al., 2000; Roumelioti & Kiratzi, 2002; Roumelioti & Beresnev, 2003). We also defined an average error (ε) for the frequency band used as

$$\varepsilon = \frac{1}{m}\sum_{j=1}^{m} E(f)_j, \tag{6}$$

here m is the number of frequencies used to calculate the average.

Table 2. Modeling parameters used for the simulation method

PARAMETER	PARAMETER VALUE
Fault orientation (strike/dip) (Degree)	270 / 67
Fault dimensions along strike and dip (km)	14, 10
Location of rupture initiation point	30.804° N, 56.734° E (BHRC)
Depth to the top of the Fault (km)	0.0
Mainshock moment magnitude (Mw)	6.4
Stress parameter (bars)	50
Subfault dimensions (km)	3.5×3.3
Subfault corner frequency (Hz)	0.53
Crustal shear-wave velocity (km/s)	3.5
Rupture velocity (km/s)	0.8 × shear-wave velocity
Crustal density (g/cm3)	2.8
$Q(f)$	$Q(f) = 130 f^{0.94}$
Windowing function	Saragoni-Hart
Geometric spreading	R^{-1}($R \le 100$ km), $R^{-1/2}$($R > 100$ km)
Crustal amplification	Boore and Joyner, 1997
Kappa (parameter of high-cut filter, sec)	0.035 & 0.030 (Boore and Joyner, 1997)

RESULTS

The free parameter, *sfact* is determined by minimizing model bias, as defined by equation 5 through a grid-search approach. It is found that a value of *sfac*t equal to 1.4 gives the best fit between simulated and observed spectra within the examined frequency range. The obtained value of subfault corner frequency (Eq. (2)) is around 0.6, which lies below the frequency range of interest (0.6–15 Hz). We also examined the relative performance of the different values of *sfact* in reproducing the target PGAs (defined as the geometric average of the two horizontal peak values) at all stations. PGA values at all the stations obtained for different values of *sfact* are tabulated in Table 3. The numbers written in bold are the closest to the corresponding average values.

In Figure 2, we present the results of the stochastic simulations and their comparisons with the observed strong ground-motion recordings. In general, the synthetics are in good agreement with observations in almost all cases, considering inherent limitations of the method and its simplicity. Large discrepancies observed at some stations (e.g., ZAR, DAV, HOR and LOL) can be attributed to insufficiencies of the generic amplification functions. Figure 3 presents the mean modeling bias for all 17 simulated WNA events.

Table 3. PGA values at selected sites for different values of *sfact*

sfact	Peak ground acceleration (cm/s/s)								
	CHT	DAS	DAV	HOR	LOL	QAD	RAV	SHI	ZAR
1.0	56	22	22	37	22	125	42	119	115
1.1	68	27	27	**44**	26	150	51	142	138
1.2	**81**	32	32	51	31	**177**	60	167	164
1.3	95	37	37	59	37	207	70	194	192
1.4	109	43	43	68	**43**	238	81	223	221
1.5	125	49	**50**	77	49	272	**93**	254	253
1.6	142	**56**	56	86	56	308	105	286	**286**
1.7	160	63.0	63	96	63	345	118	**320**	321

[1]Values typed in bold are closest to the average of observed horizontal PGA.

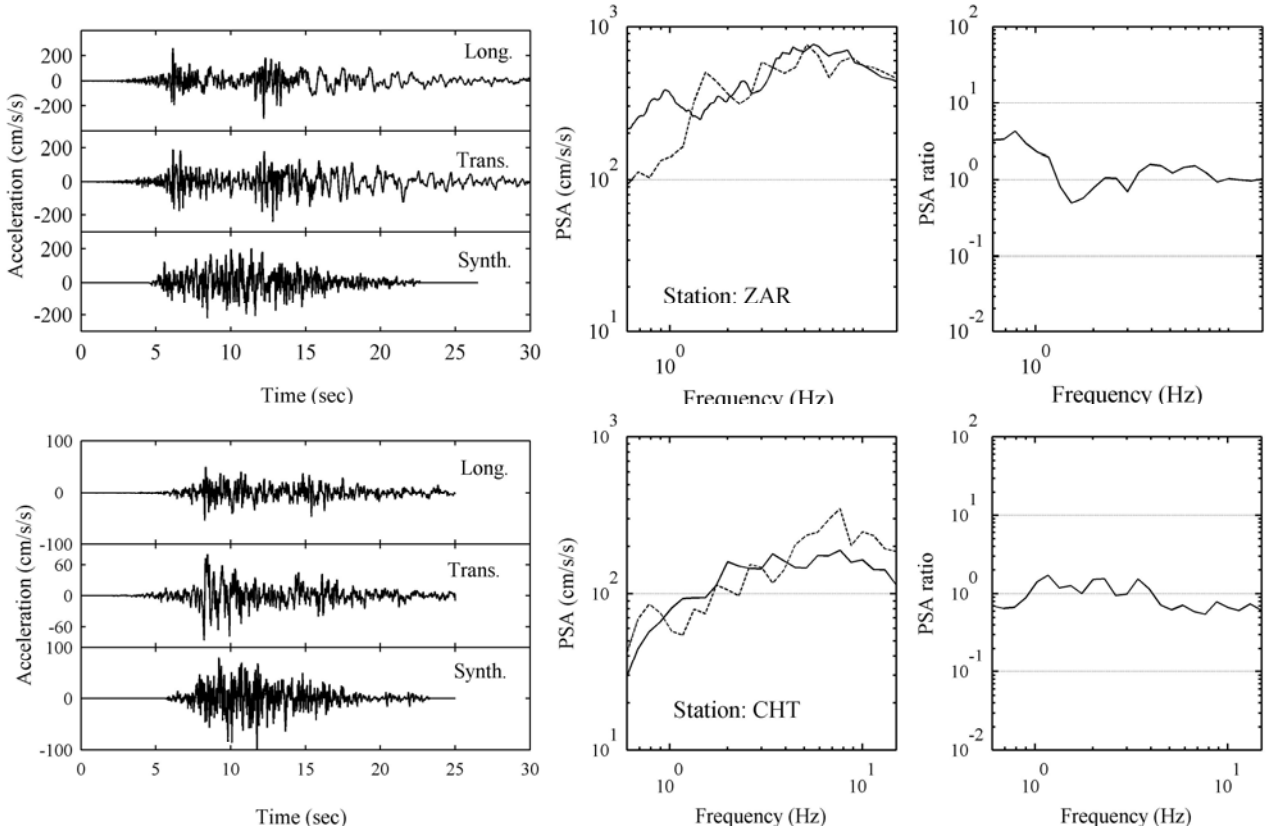

Figure 2. Comparison of the simulated acceleration time histories with observed records (left). The observed 5% damped pseudo-acceleration response spectra and the spectra simulated in this study are also shown (centre). The average spectra of the two horizontal components are shown by solid lines. Simulated spectra are shown by dotted lines. On the right Figure, the ratio of observed to simulated spectra is also shown. (Figure continues on following page)

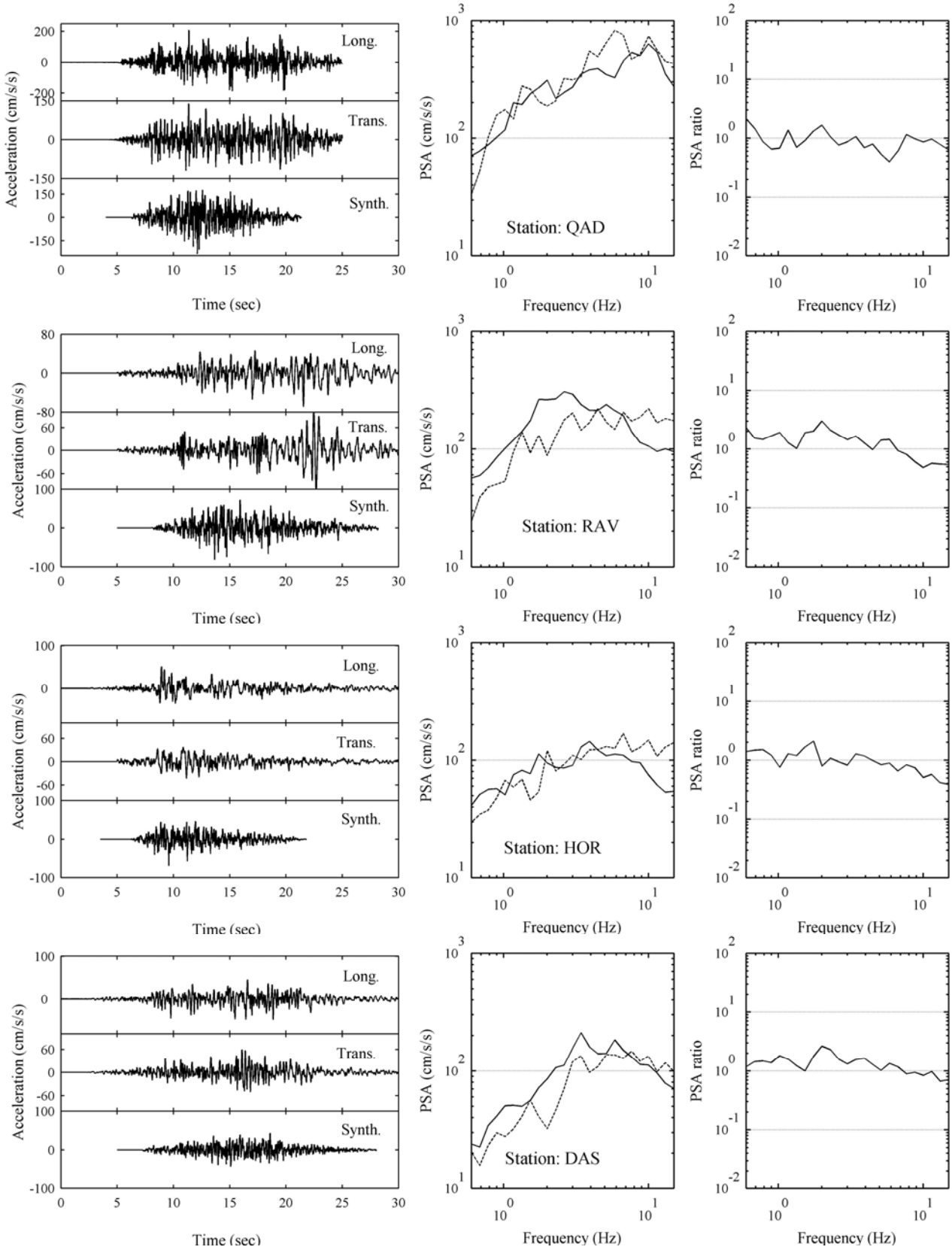

Figure 2. Continued.

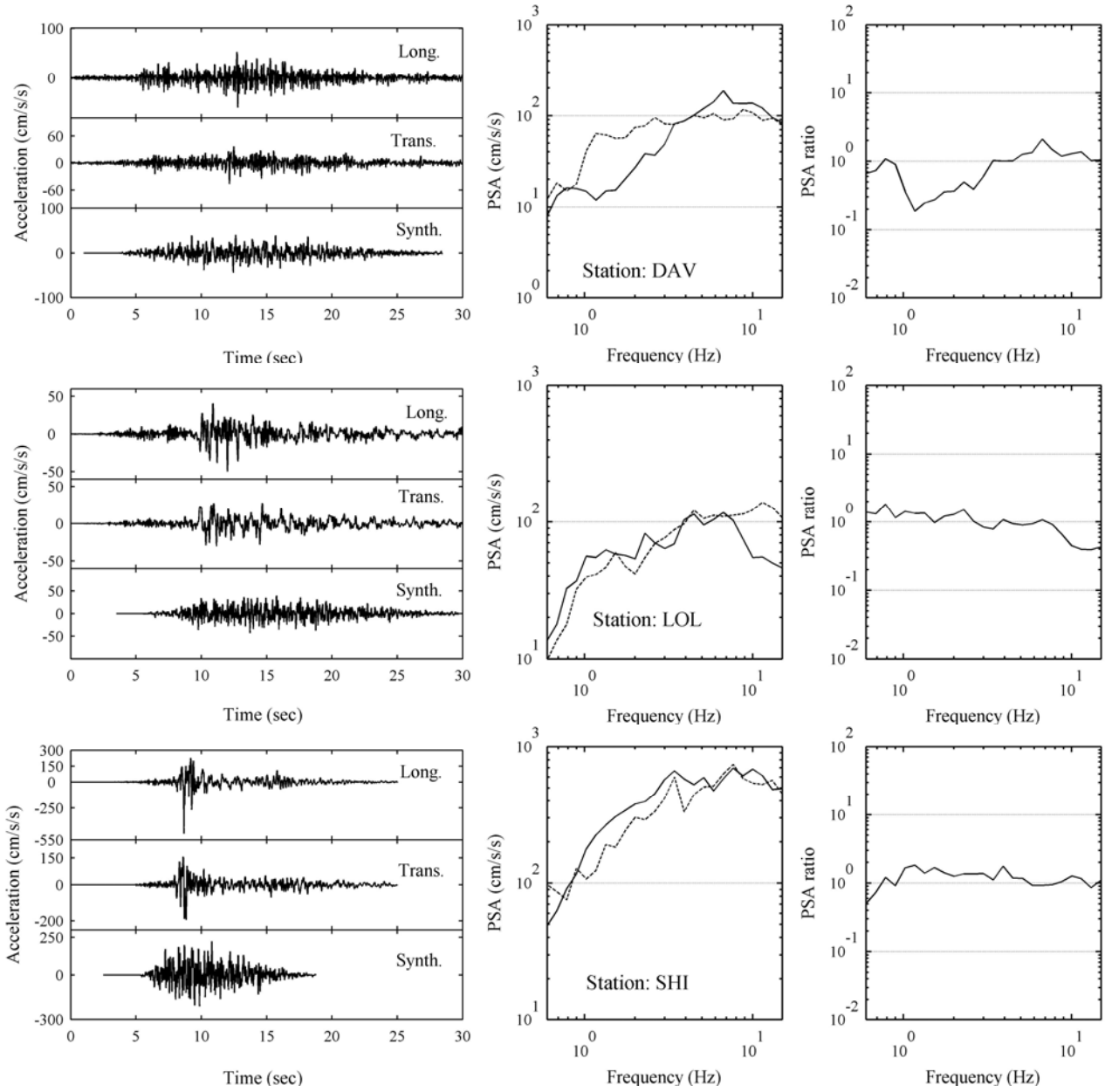

Figure 2. Continued.

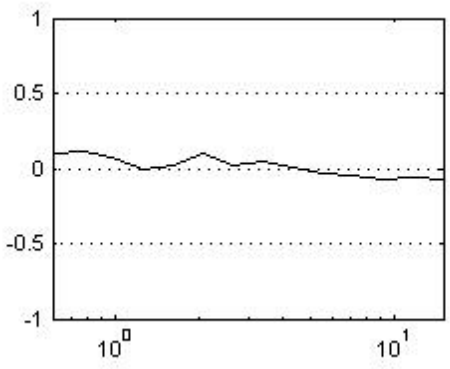

Figure 3. The bias calculated for the best value of radiation strength factor (*sfact*). We used all stations and the entire frequency band (0.6–15.0 Hz). The bias is defined as the logarithm of the ratio of the observed to simulated response spectrum, averaged over all stations (see Eq. 5).

COUNCLUSION

With regional and generic empirical relations and dividing the fault rupture into 4×3 subfaults of 3.4 km size, we find a radiation-strength factor *sfact*=1.4 (for a representative value of stress parameter $\Delta\sigma = 50$ bars). These parameters, obtained from the stochastic modeling, reproduce reasonably well the observed PSA and PGA at all distances and azimuths. Model bias calculated using equation (5) and the final model parameters listed in Table 1.

We employed mean amplification factors estimated for rock and stiff-soil sites (Boore and Joyner, 1997) to account for the effects of local site effect. The results show a satisfactory match between simulated and observed peak ground accelerations and response spectra, although significant discrepancies were observed at individual stations. These discrepancies observed at some stations (e.g., ZAR, DOV, HOR and LOL) can be attributed to insufficiencies of the site effects. Our results show that the applied method in combination with a very simplified representation of local site effects can satisfactory reproduce recorded strong ground motion of the 2005 Zarand earthquake on average. A More detailed analysis of site-specific responses is necessary to improve the shape matching of the spectra at these sites.

REFERENCES

Aki, K. and Richards P.G. Quantitative Seismology, Theory and Methods, Vol. 1. Freeman Publishing, San Francisco, CA, 1980.

Berardi R., Jimenez M.J., Zonno G. and Garcia-Fernandez M. “Calibration of stochastic finite-fault ground motion simulations for the 1997 Umbria-Marche, Central Italy, earthquake sequence”, Soil Dynamics and Earthquake Engineering, 20, 315-324, 2000.

Berberian, M. Contribution to the seismotectonics of Iran (Part II), Geological Survey of Iran, Rep. No.39, 1976.

Berberian M. “Earthquake faulting and bedding thrust associated with the Tabas-E-Golshan (Iran) earthquake of September 16, 1978”, Bulletin of the Seismological Society of America, 69, 1861-1887, 1979.

Berberian M. and Yeats R.S. “Patterns of historical earthquake rupture in the Iranian plateau”, Bulletin of the Seismological Society of America, 89, 120-139, 1999.

Beresnev I.A. and Atkinson G.M. “Modeling finite-fault radiation from the Omega-n spectrum”, Bulletin of the Seismological Society of America, 87, 67-84, 1997.

Beresnev I.A. and Atkinson G.M. “FINSIM: a FORTRAN program for simulating stochastic acceleration time histories from finite faults”, Seismol. Res. Lett., 69, 27-32, 1998a.

Beresnev I.A. and Atkinson G.M. “Stochastic finite-fault modeling of ground motions from the 1994 Northridge, California, earthquake. I. Validation on rock sites”, Bulletin of the Seismological Society of America, 88, 1392–1401, 1998b.

Beresnev I.A. and Atkinson G.M. “Source parameters of earthquakes in eastern and western North America based on finite-fault modeling”, Bulletin of the Seismological Society of America, 92, 695-710, 2002.

Boore D. and Joyner W. “Site amplifications for generic rock sites”, Bulletin of the Seismological Society of America, 87, 327-341, 1997.

Roumelioti Z. and Beresnev I.A. “Stochastic finite-fault modeling of ground motions from the 1999 Chi-Chi, Taiwan, earthquake: application to rock and soil sites with implications for nonlinear site response”, Bulletin of the Seismological Society of America, 93, 1691-1702, 2003.

Roumelioti Z. and Kiratzi A. “Stochastic simulation of strong-motion records from the 15 April 1979 (M 7.1) Montenegro earthquake”, Bulletin of the Seismological Society of America, 92, 1095-1101, 2002.

Sadeghi H., Fatemi Aghda S.M., Suzuki S. and Nakamura T. “3D velocity structure of the 2003 Bam earthquake area (SE Iran): existence of a shallow brittle layer and its relation to the heavy damages”, Tectonophysics, 417, 269-283, 2006.

Takin, M. “Iranian geology and continental drift in the Middle East”, Nature, 235, No.5334, 147-150, 1972.

Talebian, M. Biggs J., Bolourchi M., Copley A., Ghassemi A., Ghorashi M., Hollingsworth J., Jackson J., Nissen E., Oveisi B., Parsons B., Priestley K. and Saiidi A. “The Dahuiyeh (Zarand) earthquake of 2005 February 22 in central Iran: reactivation of an intramountain reverse fault” Geophysical Journal International, 164, 137–148, 2006.

Jackson J.A., Haines J. and Holt W. “The Accommodation of Arabia-Eurasia Plate Convergence in Iran”, Journal of Geophysical Research, 100, 15205–15219, 1995.

Zare M., Bard P.Y. and Ghafory-Ashtiany M. “Site characterizations for the Iranian strong motion network”, Soil Dynamics and Earthquake Engineering, 18, 101-121, 1999.